

# Characteristics of a Subgrid Model for Turbulent Premixed Flames\*

V. K. Chakravarthy<sup>†</sup> & S. Menon<sup>‡</sup>

School of Aerospace Engineering

Georgia Institute of Technology

Atlanta, GA 30332-0150

## Abstract

A modified version of the linear eddy model (LEM) for subgrid combustion is developed and used for studying the properties of turbulent premixed flames in the core region of Couette flow. The handling of the burning (diffusion/reaction) and specie transport, in this new approach, is fully deterministic. The model is, therefore, found to predict the correct laminar flame speed in the limit of zero turbulence. The effect of three dimensional eddies on scalar fields at the subgrid scales is modeled using a stochastic Lagrangian rearrangement procedure. The derivation of this procedure from the inertial range scaling laws necessitates a calibration procedure since the numerical values of the constants in these laws are unknown. The present LEM approach relates the constant needed to the coefficient of eddy viscosity that is evaluated in a LES, under the assumption of constant turbulent Prandtl and Schmidt numbers. The new approach is found to predict the turbulent flame speed with fair amount of accuracy. The chemistry is modeled using a self propagating scalar field ( $G$ -equation) approach and within the limitations of this model, LEM is found to capture the right trends in evolution of flame structure, effects of heat release and turbulence. The encouraging results obtained here warrant further research into extending this subgrid model for cases of finite rate chemistry and inclusion of thermodiffusive mechanisms such as the Lewis number effects.

## 1 Introduction

The simulation of turbulent phenomena in engineering is, in the present day greatly limited by the available

computational resources. This necessitates the development of modeling tools that would enable us to simulate these phenomena within the realm of available resources. One such approach is Large Eddy Simulation (LES) in which the large scale structure of the flow is determined by solving the governing equations that are augmented with additional (approximate) model terms to account for the effect of small scales. Dissipation of kinetic energy is the only physical phenomenon of importance in non-reacting flows that occurs at small scales. Separating these small scales and the large scales (of the size of the characteristic geometric length in the flow) is the inertial range which acts purely as an energy cascade for supplying kinetic energy to the small scales from the large scales. The near universal behavior of the inertial range along with the assumption of local small scale isotropy has aided the modeling of turbulent flows using the eddy viscosity assumption.

However, there is no universally valid form of the scalar spectrum at small scales. There exist several forms of the of scalar spectrum depending on the local Schmidt number (for species) or Prandtl number (for temperature). Independent of these parameters, scalar mixing using an eddy diffusivity, nevertheless, is often used in the present day modeling studies. This approach is severely in error in cases where scalar counter gradient diffusion occurs. Further, if the fluid is reacting, the interaction between the molecular mixing and chemical reactions occurring at smallest of the scales (Kolmogorov and Batchelor scales) have significant effects on large scale fluid/flame structure. The additional non-linearity in the governing equations in case of reactive systems also needs to be handled perhaps with greater care for accurate modeling of reacting flows.

In many practical engineering systems, combustion takes place in a regime of parameter space called the corrugated flamelet zone. The flame thickness is very small as compared to any relevant fluid dynamic length scales

<sup>†</sup> Professor, Senior Member, AIAA.

<sup>‡</sup> Graduate Research Assistant.

\* Copyright ©1997 by V. K. Chakravarthy & S. Menon. Published by the American Institute of Aeronautics and Astronautics, Inc., with permission.

(Kolmogorov length scale). In this region of parameter space, the flame is wrinkled by turbulence but the local burning is laminar. The turbulent flame consists of an ensemble of locally laminar flames whose self propagation speed (laminar flame speed) is governed by the balance between temperature and specie diffusion. The probability density function (PDF) and moment closure approaches are, at the present day, inadequate in handling the diffusion processes and hence it is difficult to predict the correct reaction rate in the subgrid when these approaches are used.

When the reaction system is dominated by one physical phenomenon, there are several models that work well. Yakhot's model [1] and Fractal models [2] (for thin premixed flames with low or no heat release) that concentrate on the kinematic structure of the flame and characterize the model in terms of incoming turbulence, Fureby and Moller model [3] which uses the turbulent reaction rate based on local turbulent and chemical time scales, are a few examples. Approaches such as these could be used to arrive (often empirically) at simple inexpensive models that, on calibration over certain regions of parameter space, could work for specific class of flows.

The Linear Eddy Mixing (LEM) model seeks to separate and model independently the effects of molecular mixing from the turbulent effects on the flame. The implementation is on a one-dimensional domain which considerably reduces the modeling cost. By carrying these one-dimensional domains in each of the LES cells to account for the effects of unresolved turbulence on scalar transport and production/destruction, this approach has been extended for use in LES [4]. The linear eddy model (LEM) is further capable of accounting for the thermodynamic effects such as volumetric dilatation, differential diffusion, viscosity variation with temperature etc. There is yet another important feature of this model that is very advantageous in modeling reacting flows once the advection (due to resolved scales) is modeled correctly. That is the adequate numerical resolution of the flame. Thin flames produce steep gradients in flow properties that could become very difficult to handle computationally if one uses finite volume or finite difference schemes. If not adequately resolved, most numerical schemes cause unphysical oscillations near the flame that threaten to destabilize the numerical solution. Generally used robust schemes usually are dissipative in nature and smear out the physical gradients, thus, artificially thickening the flame. The LEM approach handles

the scalar transport in a Lagrangian manner circumventing this problem.

The Linear eddy model has been used in several numerical combustion studies. The kinematic structure of premixed flames was modeled earlier by Menon et al. [4] and this approach was extended for modeling the kinematics of a self propagating scalar interface in a wall bounded shear flow using LES with dynamic  $K$ -equation model [5]. This study utilized the  $G$ -equation [6] which models the motion of self propagating kinematic surface (model for cold flame). A subgrid kinetic energy equation model with dynamic evaluation of the model coefficients is used as the subgrid model for momentum transport. This study proves the feasibility of an online implementation of the LEM approach in a 3D LES but asks for further research into species advection modeling and inclusion of heat release effects. Some inadequacies in the advection algorithm were overcome by Calhoun and Menon [7] in their two dimensional simulation of reacting mixing layers including effects of heat release. However, as noted in [8], the inadequacies in this advection seem to cause significant errors in premixed flames as against non-premixed flames. A modified version of the advection algorithm is reported here.

The present research seeks to validate (independently) and combine the various different modeling procedures (for each of the underlying physical phenomena) to arrive at a comprehensive modeling approach for use in LES. Using this approach, the structure of premixed flames in turbulent Couette flow at  $Re$  (based on channel width and wall velocity difference) of 20000 is analysed. Experimental data from [9] is available at that  $Re$  for validation of cold flow LES. The Couette flow has a wide core region where the mean flow is small and the turbulent intensity is nearly constant. The turbulent intensity in this region can be used as a parameter against which the flame characteristics (like turbulent flame speed, flame stretch etc.) could be characterized. Also reported here are the effects of heat release on the flame structural properties.

The flame generated turbulence is found to be a significant factor in determining the flame speed. The precise nature of its effects needs to be studied can be studied using a stationary flame problem. To this end, a premixed turbulent stagnation point flame is under study using LES. Some preliminary observations are reported here.

An eddy viscosity approach based on the model  $K$ -

equation (subgrid kinetic energy equation), discussed in section 2, is used to model momentum transport. A zero Mach number fractional step method is used to numerically integrate the LES equations on a non-staggered grid. The version of the LEM approach used here is outlined in section 3. The results are analysed in section 4 and directions for future research are discussed in section 5.

## 2 Governing equations for LES

The Navier Stokes equations on convolution with a spatial filter (after filtering), reduce to the following LES equations.

$$\frac{d\rho}{dt} + \rho \frac{\partial \bar{U}_i}{\partial x_i} = 0 \quad (1)$$

$$\frac{d\rho \bar{U}_i}{dt} = -\frac{\partial \bar{p}}{\partial x_i} + \frac{\partial \tau_{ij}}{\partial x_j} + \frac{\partial \tau_{ij}^{viscous}}{\partial x_j} \quad (2)$$

The volumetric dilatation  $\partial \bar{U}_i / \partial x_i$  is obtained from the zero Mach number approximation of the energy equation arrived at by assuming a fast acoustic time scale approximation from the equations. The physical consequence of this is to remove any gradients in thermodynamic pressure (because of infinite propagation speed). The normal stress associated with the momentum gradients (as in incompressible flows) is however spatially dependent.

For a closed set of equations, one needs to approximate the subgrid stresses using a model. The velocity variations in the scales below the characteristic filter width  $\Delta$  are unresolved in a LES. Due to the nonlinear nature of the Navier-Stokes equations, these small scale fluctuations effect the large scale motions. This effect comes from the subgrid stress, which in the present study is approximated as  $\tau_{ij} = -\frac{2}{3}\rho K \delta_{ij} + 2\mu_t \bar{S}_{ij}$ , where  $\bar{S}_{ij} = \frac{1}{2} [\partial \bar{U}_i / \partial x_j + \partial \bar{U}_j / \partial x_i]$  is the resolved strain tensor,  $\mu_t$  is subgrid eddy viscosity (to be defined later) and  $K = -\frac{1}{2}(\overline{U_i U_i} - \bar{U}_i \bar{U}_i)$  is the subgrid kinetic energy. Filtered variables are also called supergrid variables because they carry information about a variables at all length scales above the filter width (grid spacing).

A  $K$ -equation (for the subgrid kinetic energy) model [10] is used as the subgrid model. The advantage of this model is that it solves a single scalar equation for the subgrid kinetic energy which characterizes the velocity scale of subgrid turbulence. The subgrid kinetic energy

has in it terms accounting for production, transport and dissipation. It is a representation of the temporal non-equilibrium of the subgrid scales because the production does not necessarily equal the dissipation (even on an average).

A variable density version of the model (for use in zero Mach number equations) is used here. The eddy viscosity and subgrid dissipation are given as follows.

$$\mu_t = \rho C_\nu K^{\frac{1}{2}} \Delta, \quad (3)$$

$$\epsilon^{sgs} = C_\epsilon \frac{\rho K^{\frac{3}{2}}}{\Delta} \quad (4)$$

For the transport term, a gradient diffusion model based on eddy diffusivity model (with unit eddy Prandtl number) has been proposed and studied by Menon and Kim [11]. This approximation was found to adequately model the transport terms. Hence, this is used in a similar form in this study. The dynamic equation for  $K$  can now be written as:

$$\frac{\partial \rho K}{\partial t} + \frac{(\partial \rho K \bar{U}_j)}{\partial x_j} = \tau_{ij} \frac{\partial \bar{U}_i}{\partial x_j} - \epsilon^{sgs} + \frac{\partial}{\partial x_j} \left[ \mu_t \frac{\partial K}{\partial x_j} \right] \quad (5)$$

The turbulent dissipation due to compressibility and dilatational effects is assumed to be insignificant at the low Mach that are to be encountered.  $C_\nu$  and  $C_\epsilon$  are the model constants that need to be specified. These constants, however, are not universal and differ with flow fields in general. This suggests that these constants also depend on the local (supergrid) structure of the flow field. It is, then appropriate to refer to them as coefficients rather than constants. A dynamic approach is applied here to evaluate these coefficients, thus removing the arbitrariness in prescribing these coefficients. The approach is based on the concept of subgrid stress similarity supported by experiments in jets (Liu et al. [12]). In this approach, a test filter (similar to the LES filter) of characteristic width  $2\Delta$  is defined and the corresponding filtered velocity field is denoted by  $\widetilde{U}_i$ . This new velocity field is obtained by convolution of the LES filtered velocity with the test filter. The subgrid stress corresponding to the scales in between the grid filter width and the test filter width is termed the test filter stress. Assuming stress similarity between the test filter stress and the subgrid stress, along with equations similar to eq.(3) and eq.(4) the test filter variables, one can arrive

at equations for the model coefficients. These equations can be found in [13] and are omitted here for brevity.

The equations are discretized on a non-staggered grid (with spacing corresponding to the characteristic filter width  $\Delta$ ) and numerically integrated using a two step semi-implicit fractional step method. The Poisson equation in this method is solved numerically using an elliptic solver that uses a four-level multigrid scheme to converge the solution. The species transport between cells is handled in a Lagrangian manner and thus the species equation need no integration on the supergrid level.

### 3 Linear Eddy subgrid model

A subgrid modeling approach based on linear eddy mixing model (Kerstein, [14-17]) was proposed by Menon et al. ([18],[19],[20]). In this approach, the turbulent stirring of the scalar field and molecular diffusion (leading to laminar propagation) are accounted for distinctly. The effects of each of these phenomena on flame characteristics can hence be studied in isolation. The modeling procedure with appropriate justification is presented here in brief.

The subgrid modeling is conducted on a one-dimensional domain (in each of the LES cells) representing a ray of length  $\Delta$  across the turbulent flame brush. This domain is divided into number (specification to be explained later) of cells each representing a finite volume with the total volume adding upto the volume of the LES cell.

A field equation for self propagating scalar interface called the  $G$ -equation [6] is used to model the laminar flame propagation in this study. This equation is designed to propagate a scalar interface at the laminar flame speed in stagnant flow and has the following form.

$$\frac{\partial G}{\partial t} = S_l |\nabla G| \quad (6)$$

For the case of moving fluid, the interface also gets convected along with self propagation and a convection term needs to be added to the above equation.

The scalar  $G$  here, is a representation of the rate of advancement in a premixed reaction. It has a binary representation on the subgrid one-dimensional domain (later referred as the linear eddy domain).  $G = 1$  represents an unburnt state and  $G = 0$  represents a burnt state on each LEM cell. The interface between two dissimilar adjacent cells is considered to be an infinitely thin flame

that propagates into the unburnt zone at a specified flame speed. The temperature rise due to the reaction is modeled by assuming the temperature to be a linear function of  $G$ . In this way, the  $G$ -equation replaces the reaction-diffusion equations for both species and temperature (that, in conjunction make the premixed flame self propagating). In the burnt state, the temperature rises to the prescribed value of the product temperature. Since the thermodynamic pressure is assumed to be constant (which is the case across premixed flames governed by second order chemical kinetics), the density varies inversely with temperature. Since the transport and diffusive properties of  $G$  and temperature would be closely correlated in this approach, it is to be assumed that these simulations correspond to a case of constant  $Le$  (Lewis number), specifically 1.0.

As can be seen in the above equation, the  $G$ -equation does not include any convective term. The effect of subgrid velocity (turbulence) is modeled separately using a stochastic process. A Lagrangian rearrangement is used to model the effect of fluid dynamic eddies on the scalar field. The length scale of the eddy (segment size on which this rearrangement process is to be conducted) and the frequency of stirring at that length scale are determined using isotropic inertial range (assumed to exist in the subgrid scales of the LES) scaling laws. There is no universality of the rearrangement scheme. It can be arbitrary but it should mimic the effect of hydrodynamic eddies on the scalar field and be conservative (retain the lowest scalar moments invariant).

A triplet map [17] is chosen for the present study. In this mapping, the chosen segment is divided into three equal parts. All spatial gradients are increased by a factor of 3 in the portions at the ends, and a factor of -3 in the middle portion. The scalar field in the three segments is pieced together to give a continuous scalar field with scalar values at the end points of the segment remaining the same as before and the scalar gradients increased by 3 times in magnitude (as illustrated in [5]). These increased gradients cause increased scalar diffusion in accordance with what has been observed as the effect of turbulence on scalar transport and dispersion. The number of finite volume cells in each subgrid domain is so chosen that a stirring event at the smallest relevant (energetic possessing) scale could be implemented. This is assumed to be the Kolmogorov length scale  $\eta$ . A line segment needs to have atleast 6 cells to implement a triplet map, so the cell size should be no less than  $\eta/6$ .

So the total number of cells is  $6\Delta/\eta$ .

The triplet map causes particle dispersion with mean square displacement of  $4l^2/27$ , where  $l$  is the length of the segment. The diffusivity associated with such a process would be  $2\lambda l^3/27$ , where  $\lambda$  is the frequency per unit length. The diffusivity due to turbulence for all length scales below  $l$  can be determined from the inertial range scaling laws (relevant dimensional analysis) in terms of the  $\eta$ ,  $l$  and  $\nu$ . It can be shown that it has the same form as eddy viscosity at that length scale, only difference being the constant of proportionality is now  $C_\nu/Pr_t$  instead of  $C_\nu$ .  $C_\nu$  is determined as explained in the earlier section and it is assumed that  $Pr_t$  is 1.0. Thus the constant of proportionality is arrived at from analytical reasoning rather than a calibrating procedure undertaken in [7]. Equating the value of diffusivity to the corresponding integrated effect of triplet mappings at various length scales, one can arrive at the PDF for length scale  $l$  and the stirring frequency (using the procedure adopted in [5]). The stirring procedure in conjunction with the molecular diffusion has been shown to effectively model the effect of three dimensional inertial range turbulence on the scalar fields [21].

Advection due to the supergrid velocity brings about transport of chemical species from one LES cell into its neighbouring cells. This is modeled using a procedure termed as “splicing” [17]. The scalar flux across each LES cell face is computed using the filtered velocity on the cell face. The number of subgrid cells corresponding to the scalar flux are transferred from one cell to its neighbour across the cell face in accordance with the direction of the scalar flux.

Instead of picking these cells from a random location on the donor subgrid domain like in the earlier research [5], cells are transferred from one end of the subgrid domain. The cells that are spliced in are put at the opposite end of the domain. In time, the linear eddy cells to be spliced in first get spliced out first. In the laminar limit (achieved by removing stirring), the flame travels from one end to another end of the cell at the rate of  $S_l$ , the laminar flame speed. When a LES cell is fully burnt the flame crosses over to the next LES cell and this process is found to predict the right laminar flame speed on the supergrid (on an average). The earlier splicing algorithm with randomly chosen locations for transfer of subgrid segments does not ensure this. Further, the introduction of cells spliced into the receiver subgrid domain can cause extra flames at the interface (between the cells put

in and the existing cells). The splicing algorithm models advection and is not supposed to create any scalar gradients (flames in the present case) on the linear eddy domain. So, in the event of an artificial flame being created at the interface, the spliced in cells are rearranged to remove this extra flame. The only exception to this procedure is the case of burning initiation in a fully unburnt cell in which case one flame caused at the interface is retained. This procedure prevents the existence of more than one flame in laminar flows (there is no flame brush in laminar flames). This approach was found necessary to obtain the correct laminar propagation on the supergrid especially in case of curved flames (cylindrical and spherical). In the turbulent case, the stirring could cause multiple flames to exist on the same subgrid domain and this could be interpreted as a stochastic representation of flame brush in each cell.

Finally the average density along the subgrid domain is used as the filtered density on the supergrid and is used to compute the volumetric dilatation on the supergrid.

## 4 Results and Discussions.

The LES numerical code is validated against the experimental results obtained from turbulent Couette flow experiments [9]. Shown in fig. 1 and fig. 2, respectively, are the profiles of mean velocity and *rms* of axial velocity for Couette flow at Re of 20000. A 49x49x33 is utilized for this simulation. Hyperbolic tangent stretching is used for the grid spacing along the wall normal direction. As can be seen, the mean velocity profile is anti-symmetric about the centre-line where as the experimental prediction is not. It was argued that this does not cause any bias in the  $u'$  profile which is in fact found to be symmetric. The peak in  $u'$  profile is much closer to the walls in experimental data than in the LES. The cause of this discrepancy is unknown. It is likely that the wall layer needs more resolution or the experimental results may be in error due to moving wall (belt) vibrations which make the flow noisy. This LES approach has earlier been validated by simulating turbulent Couette flow at Re of 5200 by comparing with experiments in [5].

In order to ease the implementation of LEM on LES grid, the mid 78 percent of the grid is made uniform. The simulations are stopped once the flame reaches the boundaries of this uniform region. The capability of linear eddy subgrid model in capturing thin flames is illustrated in fig. 3. For comparison, starting with the

same initial conditions, LES is conducted using a finite difference implementation of  $G$ -equation with turbulent flame speed obtained using the Yakhot's model [1]. Nine contours corresponding to nine equally spaced values of  $G$  are shown in fig. 3. The finite difference implementation of chemistry is seen to thicken the flame front, thus, reducing the gradients. This in turn causes a reduction in flame speed. As was sought from the conclusions of earlier LEM research [5], the linear eddy model (with the new advection modeling approach) now propagates the laminar flame on the supergrid at the correct flame speed for both planar and spherical flames. This removes the arbitrariness in advection algorithm [5] and the calibration procedure for diffusion/burning [7]. The turbulent stirring becomes the only stochastic part of the approach and the only arbitrariness is in prescribing  $Pr_t$ .

The premixed flame propagation is simulated for values of  $u'/S_l$  : 1.0, 4.0 and 8.0. For all these cases, simulations are conducted for three different values of product temperatures ( $T_p$ ).  $T_p/T_f$  of 1.0, 4.0 and 7.0 are used. So there are nine cases in the parameter space. Since the flames are not stationary, one needs several realizations of the flow at the same time after ignition for statistical analysis. For each of the above cases, several LES realizations (starting from different realizations of non-reacting flow LES as initial conditions before igniting the flame) of the flow are simulated till the statistics converge.

The temporal evolution of the flame structure is discussed first, followed by analysis of effects of increasing relative (to  $S_l$ ) turbulent intensity. Since the cold flames have been studied earlier, this analysis is done for flames in the presence of heat release. The effects of increasing heat release are discussed later.

The local structure of the flame can be characterized using the principle radii of curvature. These are computed from the eigen values of the curvature tensor [22]. The ratio of smaller radius to the higher, is referred to as the shape factor. It lies between -1 (corresponding to a saddle point) and 1 (spherical shape). The value of 0 corresponds to a cylindrical shape. The hydrodynamic effects on the flame are mainly characterized by two quantities, the tangential strain rate in the plane of the flame and the flame stretch which is defined as the rate of change of a Lagrangian flame surface at a given location. Mathematical means of computing these quantities can be found in [22]. The strain rate gives an estimate of the hydrodynamic force acting in the plane

of the flame. The flame stretch determines the rate at which the flame is deforming with the effects of self propagation included. Positive stretch indicates a tendency of the flame to replanarize thus reducing the curvature and hence also the turbulent flame speed. In the limit of a material surface ( $S_l = 0$ ), the tangential strain rate and the flame stretch are highly correlated. Probability density functions (PDFs) of each of these local flame properties are constructed in order to characterize the gross nature of the flame. The strain rate and flame stretch are non-dimensionalized using the Kolmogorov time scale and the curvature is non-dimensionalized using the integral length scale (prescribed).

In fig. 4, the transition from a spherical to (locally) cylindrical nature of the flame is shown for the case of  $u'/S_l$  of 8.0 and  $T_p/T_f$  of 7.0. When the fuel is ignited at a point source, the initial growth is (globally) spherical. With increasing time the effect of turbulence is realized in terms of wrinkles that are characterized by increase in shape factor PDF near cylindrical zone. Eventually the effect of mean velocity comes in and elongates the flame and the turbulence wrinkles the flame front. This is illustrated graphically to a certain extent in fig. 5. Then the flame becomes mostly cylindrical and finally, towards the end of the simulation, some saddle nature is noticed. This trend of PDF shifting towards the saddle zone from mostly cylindrical nature (once the effect of turbulence is fully realized) is also noticed as the shear layer evolves spatially in [22]. In fig. 6 is shown the evolution of flame stretch PDF with time. The time here is non-dimensionalized by the total time of the simulation (just before the flame leaves the domain where LEM is implemented). For an outward burning hot flame, the curvature and volumetric dilatation (expansion) are always positive leading to positive flame stretch. As the flame expands, the curvature effect reduces and turbulence effect is felt more. In isotropic turbulence, the stretch is nearly symmetric except that the self propagation contribution skews the PDF slightly towards the positive side. This skewness reduces with increasing  $u'/S_l$  and PDF is very nearly symmetric for material surfaces [23]. The flame is indeed found to transition towards this nature gradually from its initial state of fully positive stretch.

The simulations with  $T_p/T_f$  of 7.0 are analyzed to study the effects of reducing  $S_l$  with same  $u'$  (increasing  $u'/S_l$ ). The tangential strain rate PDFs for three cases of  $u'/S_l$  are shown in fig. 7. Increasing the flame speed causes the negative curvature to decrease and positive

curvature (concave to the fuel side) to increase. Due to positive volumetric dilatation on the burnt side, regions of positive curvature experience high strain rates on the surface. So the PDF is more skewed to the right for the case of higher  $S_l$ . Alternately, as turbulence intensity increases relative to  $S_l$ , the nature of the flame tends more towards that of a material surface thus reducing the skewness. As noticed in earlier studies [22] involving spatial mixing layers, the mean curvature PDF (fig. 8) is slightly shifted to the right (because of finite  $S_l$ ) and is found to be independent of  $u'/S_l$ . The flame stretch (fig. 9) is found to behave in much the same fashion as the tangential strain rate because the curvature remains unchanged. Because of slight positive skewness in curvature PDF, it is easy to see from the expression for flame stretch, that the flame stretch skewness is slightly reduced as compared to flame strain rate.

The relative alignment of the flame normal with the direction of most compressive strain rate (eigen vector corresponding to the lowest eigen value of the strain tensor) is computed and plotted in fig. 10. Contrary to the previous reports [24] of the PDF peak at an alignment angle of  $30^\circ$  in shear driven flows, the peak is closer to  $0^\circ$  indicating a tendency of the flame normal to align with the compressive strain rate direction. This was observed in isotropic turbulence simulations earlier [24]. Two reasons could perhaps be attributed for this behavior. First, the mean shear is very small in the core region and hence the turbulence may be close to being locally isotropic. Second, in the presence of heat release, the mean shear effect may be insignificant because the flow is modified drastically due to density changes. The volumetric dilatation tries to accelerate the flame propagation thus trying to compress the flame brush. In such cases, the higher two eigenvalues are both most likely positive thus making the tangential strain rate highly positive for high heat release cases as noticed in fig. 7.

The effects of increasing heat release on the flame structure are analyzed using cases with  $u'/S_l$  of 4.0. The tangential strain rate is plotted, for the three values of heat release under consideration, in fig. 11. As seen earlier, the most compressive principle strain rate aligns closely with the flame normal at most of the points. The sum of the three principle strains is positive and increases with increasing heat release. Since the strain rate normal to the flame is negative, it is very likely that the two higher values of the principle strain rates are positive leading to an overall positive strain rate in the

plane of the flame. Mean curvature (shown in fig. 12) is slightly biased towards the positive side. The likelihood of regions on the flame with higher mean curvature is found to increase with heat release. The heat release causes faster flame growth due to dilatation but this acceleration could dewrinkle the flame, thereby reducing the local radii of curvature (increasing curvature). The flame stretch is plotted in fig. 13 and is found to correlate well with the behavior of the tangential strain rate since the curvature is nearly symmetric.

The turbulent propagation rate of the premixed flames, while they are in the core region, is characterized against the turbulent intensity of the cold flow into which the flame is propagating. The turbulent flame speed predictions (experimental and theoretical) exhibit a large amount of scatter. The key reason for this being the fact that there may be parameters that are different in various studies and, hence, comparing the results from these to arrive at some definite conclusions cannot be rationalized. Bradley et al. [25] in their survey of available of experimental results for characterizing turbulent flame speed against inflow turbulence, found it necessary to consider the dimensionless Karlovitz stretch factor as a relevant parameter. It is a measure of chemical time against the eddy time and is given as [26]:

$$K = 0.157 \left( \frac{u'}{S_l} \right)^2 R_l^{-0.5} \quad (7)$$

where  $R_l$  is the turbulent Reynolds number based on the integral length scale.

The results reported were therefore separated into different zones depending on the value of this parameter times the Lewis number. They report results that fall into two zones corresponding to mean values of  $K.Le$  values of 0.1 and 1.0 with a scatter of about 25 percent. Some of these experimental results are plotted along with the predictions from the current study in fig. 14. The values of the above mentioned parameter are 0.01, 0.15 and 0.46 respectively for  $u'/S_l$  values of 1.0, 4.0 and 7.0. Also included are the best fit lines to experimental predictions at  $K.Le$  of 0.1 and 1.0. It is found that the cold flame front propagation matches the experimental data rather well. However, the turbulent flame propagation is much faster in cases with heat release. The compounded effect of two factors could be the reason for the observed increase with heat release. Flames that are primarily convex (burning outwards from burnt side) experience some amount of outward acceleration. The

countering effect would be that this increases the flame stretch thus reducing the flame speed. Also, a wrinkled exothermic propagating front generates some fluid dynamic disturbances which in turn change the flame propagation speed. These disturbances (termed flame generated turbulence) add onto the incoming turbulence and one can define an “effective turbulence intensity” [26] that determines the flame structure. Leisenheimer and Leuckel [27] were able to measure this effective intensity in a premixed flame propagating radially. Radial symmetry (in their study) on an average allowed for decomposition of the flow into an average field and turbulence. There is no way of studying this phenomenon using an arbitrary non-stationary flames and is left as an objective for future research.

The LEM approaches is being currently used to simulate turbulent premixed stagnation point flows. This flame is stationary and also is two-dimensional on an average. This presents one with opportunity to study, statistically, several phenomena in turbulent combustion at a lowered computational expense. A 65x49x33 grid is being used to simulate this flow on a domain that is 70mm x 200mm in wall normal and lateral directions. The width in the third direction is set at 70mm. The inflow velocity is 5.0m/s with 10.0 percent turbulence. These parameters are being used with an aim of simulating the flames studied in [27].

With the conditions being used, the turbulent flame speed turns out to be about 4 times the laminar flame speed (for  $S_l = u'$ ) which is unusually high. It is found that this could be reduced by decreasing the frequency of stirring (when put to zero, the LEM predicts the laminar flame speed). The reason for stirring being higher than required is that the subgrid kinetic energy that determines the frequency, is probably not being predicted correctly. The inflow subgrid is set at 0.1 times the turbulence level rather arbitrarily and this may be in error.

The increased stirring rate in LES of stagnation point flame is found to reduce the wrinkling of the flame on the supergrid. Some 3-dimensional wrinkling is nevertheless seen in fig. 15. Contours corresponding to  $G$  level of 0.5 are plotted for several locations along the homogeneous direction in fig. 16. Instantaneous burning is found to occur in supergrid cells that are within two grid points distance from the mean position of the flame. This indicates that the LEM approach is able to capture the flame brush in just a few grid prints.

## 5 Conclusions

In summary, it can be concluded that the modified advection algorithm overcomes the inadequacies noted in earlier research. The linear eddy subgrid approach, in the absence of turbulent stirring, is found to model laminar flame propagation correctly. In the presence of stirring (the only non-deterministic part of the approach), it is found to also predict the turbulent flame speed with fair amount of accuracy. The trends in evolution of the spatial structure of the premixed flames are also in agreement with experimental and DNS predictions. The present approach is however limited by the  $G$  equation and the corresponding state equation for temperature. The LEM needs to be extended to flames involving real chemical kinetics in order to account for effects of thermodiffusive mechanisms. Also intended for future research is the subject of flame generated turbulence. The preliminary results from LES of premixed flames in stagnation point flames are found to be quite encouraging. In fact, this problem could provide the platform necessary for studying flame generated turbulence.

## Acknowledgements

This research was supported by the NASA Lewis Research Center under Grant no. NAG3-1610.

## References

1. Yakhot, V. (1988) “Propagation velocity of premixed turbulent flames”, *Combust Sci. Tech.*, **60**, 443-450.
2. Menon, S. and Kerstein, A. R. (1992) “Stochastic simulation of the structure and propagation rate of turbulent premixed flames”, *Twenty fourth symposium (Int.) on combustion*, The Combustion Institute, 443-450.
3. Fureby, C. and Moller, S.-I. (1995) “Large eddy simulation of reacting flows applied to bluff body stabilized flames”, *AIAA J.*, **12**, 2339-2347.
4. Menon, S., McMurtry, P. A., and Kerstein, A. R. (1993) “A linear eddy subgrid model for turbulent combustion: Application to premixed combustion”, *AIAA paper 93-0107*, *AIAA 31<sup>st</sup> Aerospace Sciences Meeting*.
5. Menon, S. and Chakravarthy V. K. (1996) “Large eddy simulation of premixed flames in Couette flow”,

*AIAA paper 96-3077, 32nd AIAA/ASME/SAE/ASEE Joint Propulsion Conference.*

6. Kerstein, A. R., Ashurst, W. and Williams, F. A. (1988) "Field equation for interface propagation in an unsteady homogeneous flow field", *Physical Review*, **A37**, 2728-2731.
7. Calhoun, W. H. and Menon, S. (1997) "Linear-eddy subgrid model for reacting large eddy simulations: heat release effects", *AIAA paper 97-0368, AIAA 35<sup>th</sup> Aerospace Sciences Meeting*, Reno.
8. Smith, T. M. and Menon, S. (1997) "Large-eddy simulation of turbulent reacting stagnation point flows", *AIAA paper 97-0372, AIAA 35<sup>th</sup> Aerospace Sciences Meeting*.
9. Menon, S., Disseau, M., Chakravarthy, V. K. and Jagoda, J. (1997) "Turbulent premixed flame propagation in microgravity", *Proceedings of the Fourth International Microgravity Combustion Workshop*, 155-160.
10. U. Schumann. (1975) "Subgrid scale model for finite difference simulations of turbulent flows in plane channels and annuli", *J. Comp. Phys.* **18**, 376-404.
11. Menon, S., and W.-W. Kim. (1996) "High Reynolds number flow simulations using the localized dynamic subgrid scale model", *AIAA Paper 96-0425, 34<sup>th</sup> Aerospace Sciences Meeting and Exhibit*.
12. Liu, S., Meneveau, S. and J. Katz (1994) "On the properties of similarity subgrid scale models as deduced from measurements in a turbulent jet", 1994, *J. Fluid Mech.*, **275**, 83.
13. Nelson, C. C. (1997) "Simulation of spatially evolving compressible turbulence using a local dynamic subgrid model", Ph.D thesis (in preparation).
14. Kerstein, A. R. (1988) "Linear eddy model of turbulent scalar transport and mixing", *Combust. Sci. Tech.*, **60**, 391-421.
15. Kerstein, A. R. (1989) "Linear eddy model of turbulent transport II. Application to shear layer mixing", *Comb. Flame*, **75**, 397-413.
16. Kerstein, A. R. (1990) "Linear eddy model of turbulent transport III. Mixing and differential molecular diffusion in round jets", *J. Fluid. Mech.*, **216**, 411-435.
17. Kerstein, A. R. (1991) "Linear eddy model of turbulent transport. Part 6:i Microstructure of diffusive scalar fields", *J. Fluid. Mech.*, **231**, 361-394.
18. Menon, S. (1991) "A new subgrid model for large eddy simulations of turbulent reacting flows", *QUEST Technical Report No. 535, NASA Contract No. NAS2-13354*.
19. Menon, S., McMurtry, P. A. and Kerstein, A. R. (1994) "A linear eddy mixing model for LES of turbulent combustion", in *LES of Complex Engineering and Geophysical flows* (Galerpin, B. and Orszag, S. ed.), Cambridge Univ. Press.
20. McMurtry, P. A., Menon, S., and Kerstein, A. R. (1992) "A subgrid mixing model for LES of non-premixed turbulent combustion", *AIAA paper 92-0234, AIAA 30<sup>th</sup> Aerospace Sciences Meeting*.
21. Smith, T. M. and Menon, S. (1997) "One-dimensional simulations of freely propagating turbulent premixed flames", accepted for publication in *Combust. Sci. and Tech.*.
22. Smith, T. M. and Menon, S. (1996) "The structure of premixed flames in a spatially evolving turbulent flow", *Combust. Sci. and Tech.*, **119**, 77-106.
23. Yeung, P. K., Girimaji, S. S. and Pope, S. (1990) "Straining and scalar dissipation on material surfaces in turbulence: Implications for flamelets", *Combustion and flame*, **79**, 340-365.
24. Ashurst, Wm. T., Kerstein, A., Kerr, R. M. and Gibson, C. H. (1987) "Alignment of vorticity and scalar gradient with the strain rate in simulated Navier-Stokes turbulence", *Phys. Fluids A*, **30**, 77-106.
25. Bradley, D., Lau, A. K. C. and Lawes, M. (1992) "Flame stretch rate as a determinant of turbulent burning velocity", *Phil. Trans. R. Soc. London. A*, **338**, 359-387.
26. Leisenheimer, B. and Leuckel, W. (1996) "Self-Generated Acceleration of confined deflagrative flame fronts", *Combust. Sci. and Tech.*, **118**, 147-164.
27. Cho, P., Law, C. K., Cheng, R. K. and Shepherd, I. G. (1988) "Velocity and scalar fields of turbulent premixed flames in stagnation flow", *Twenty second symposium (Int.) on combustion*, The Combustion Institute, 739-745.

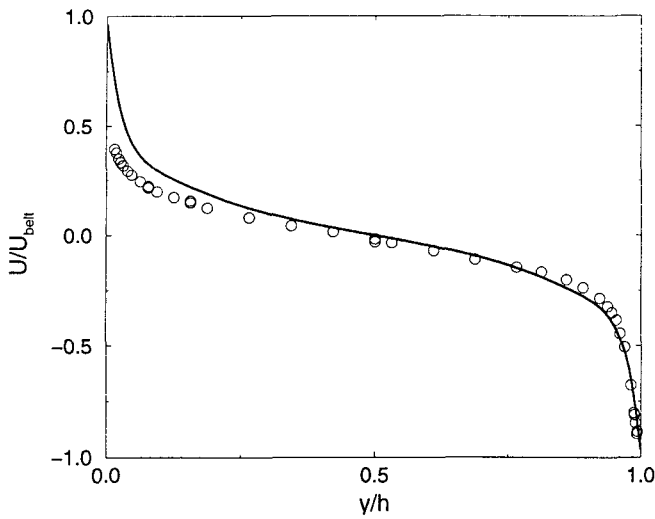


Figure.1 : Mean velocity profile in turbulent Couette flow.  
Solid line : LES, symbols : experiments [9]

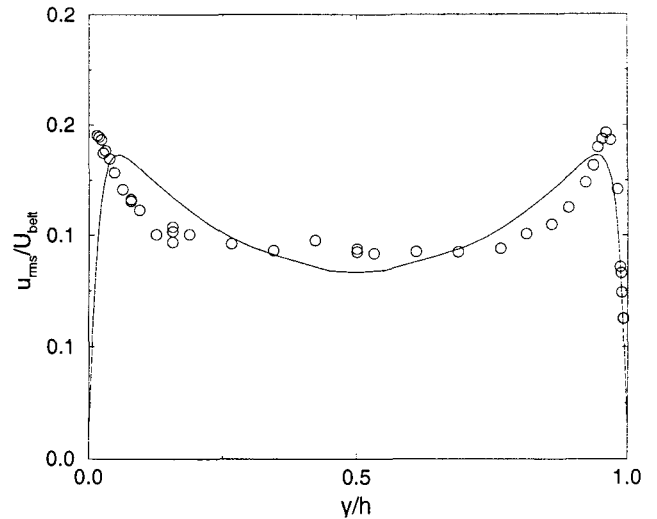


Figure.2 : Axial rms velocity profile in turbulent Couette flow.  
Solid line : LES, symbols : experiments [9]

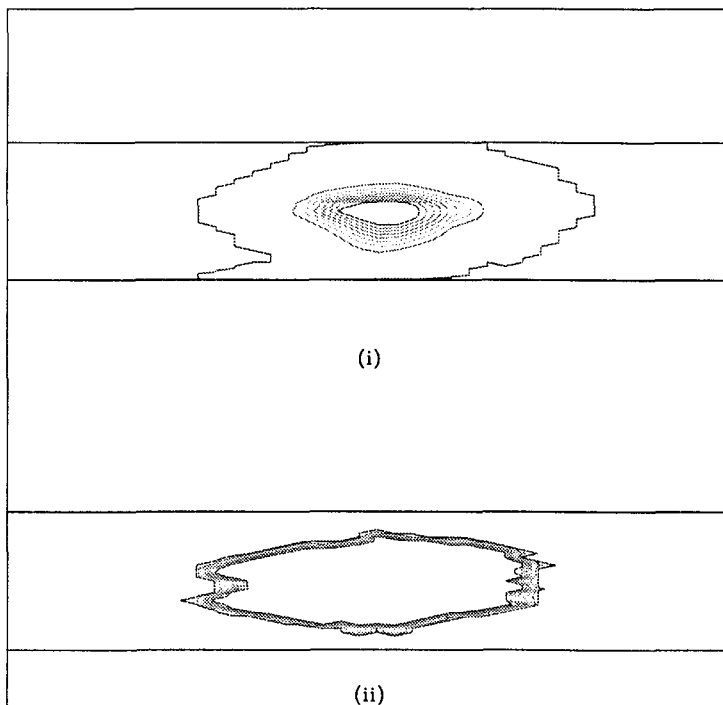


Figure.3 : G-level surface contours.  
(i) Finite difference method, (ii) LEM

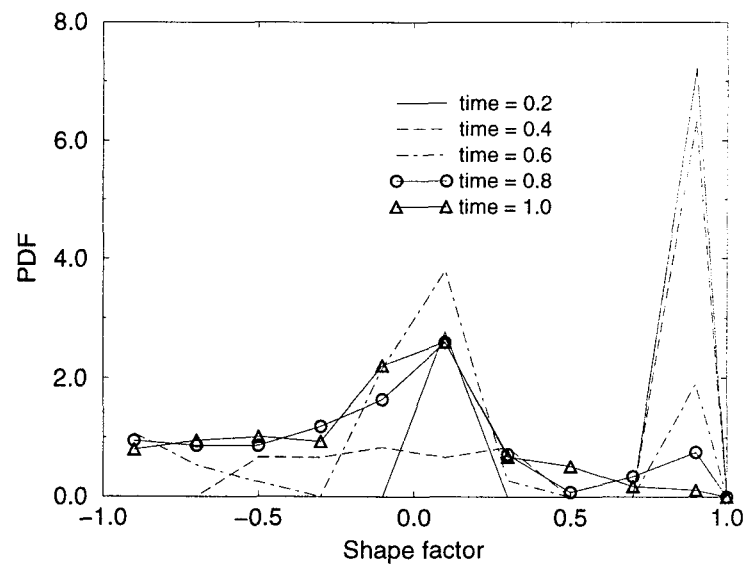
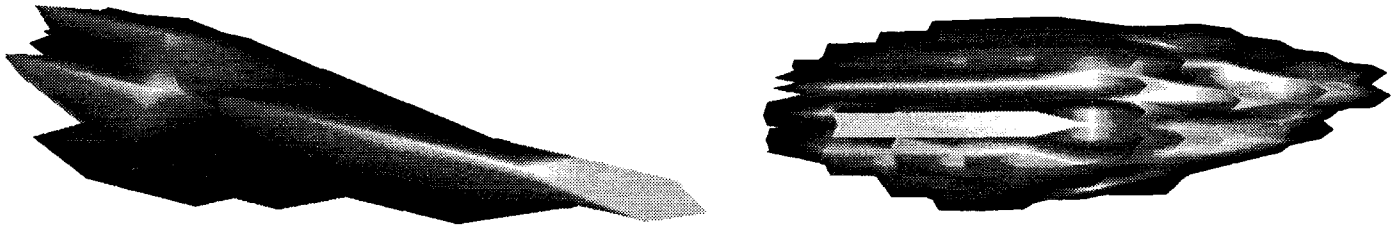


Figure.4 : LEM predicted temporal evolution of flame structure.



(i)

(ii)

Figure.5 : Geometry of the flame surface.  
(i)  $t = 0.6$ , (ii)  $t = 1.0$

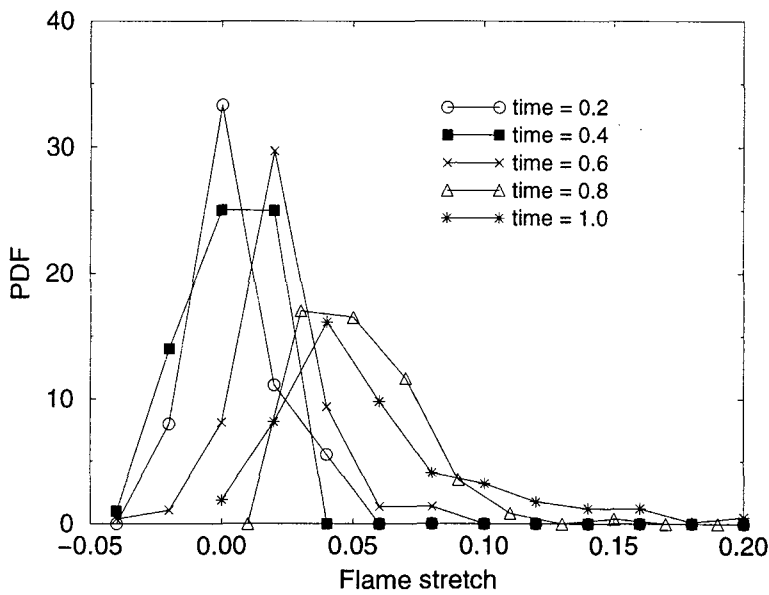


Figure.6 : Evolution of flame stretch in time.

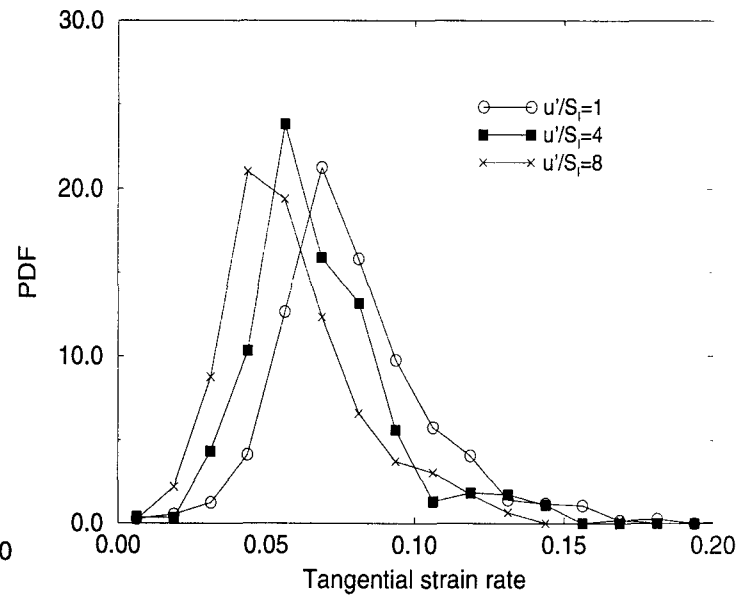


Figure.7 : Effect of laminar flame speed (relative to a constant turbulence level) on the tangential strain rate.

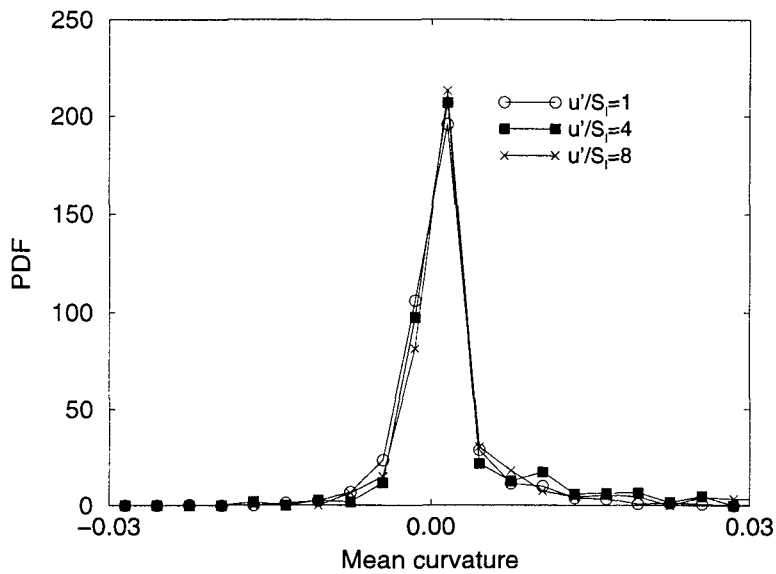


Figure.8 : Effect of laminar flame speed (relative to a constant turbulence level) on the mean curvature.

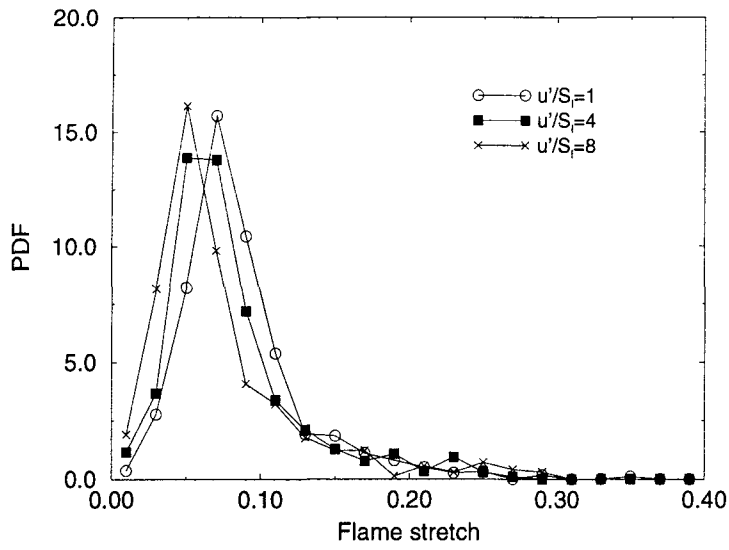


Figure.9 : Effect of laminar flame speed (relative to a constant turbulence level) on the flame stretch.

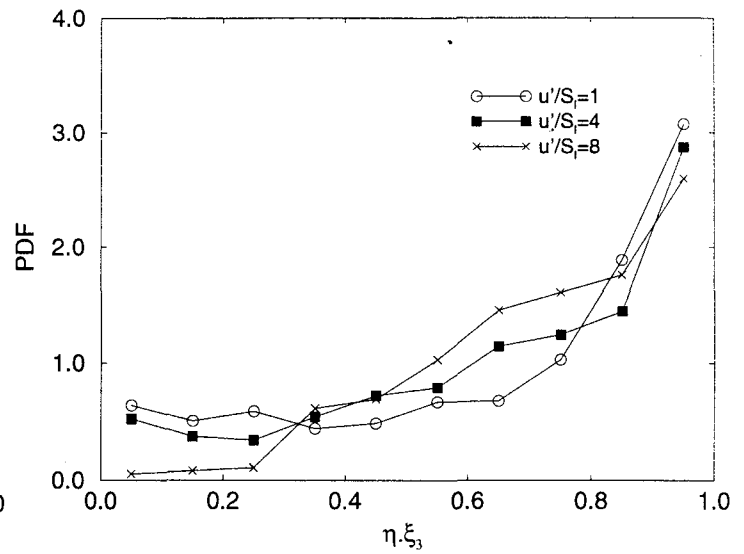


Figure.10 : Effect of laminar flame speed (relative to a constant turbulence level) on the flame normal alignment relative to the most compressive strain direction.

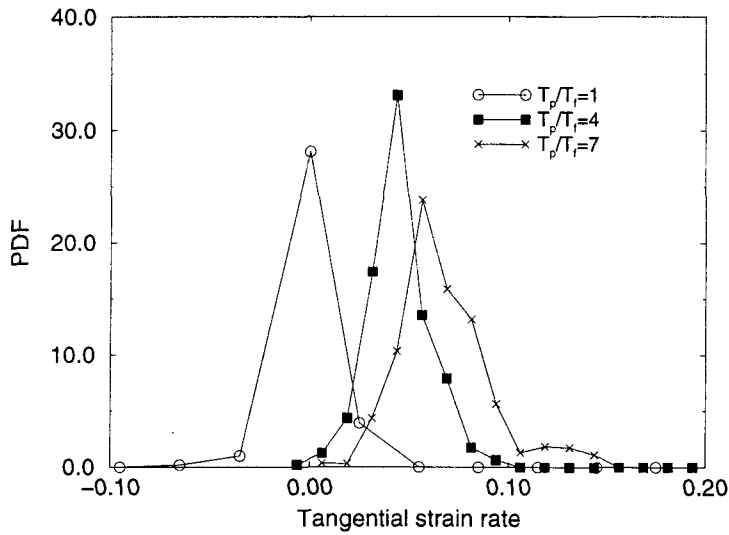


Figure.11 : Effect of heat release on the tangential strain on the flame surface.

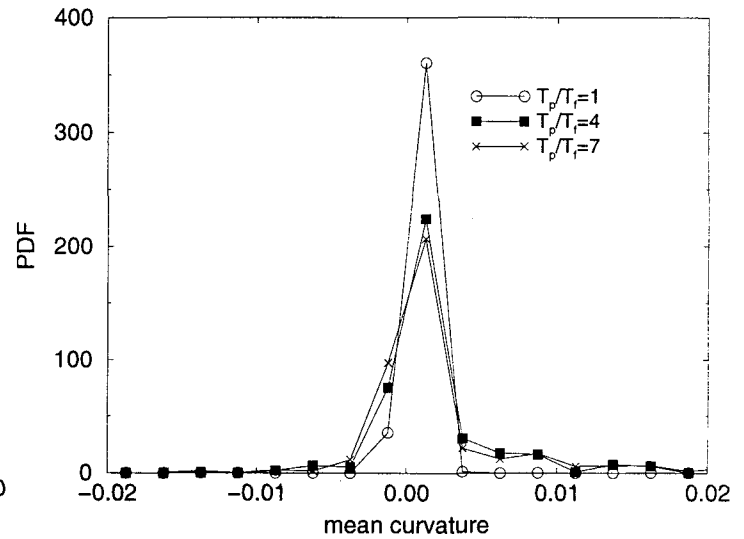


Figure.12 : Effect of heat release on mean curvature of the flame surface.

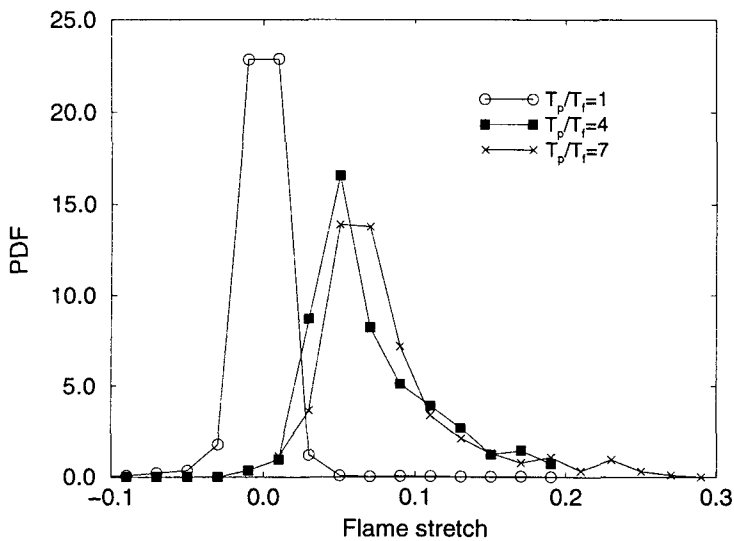


Figure.13 : Effect of heat release on flame stretch.

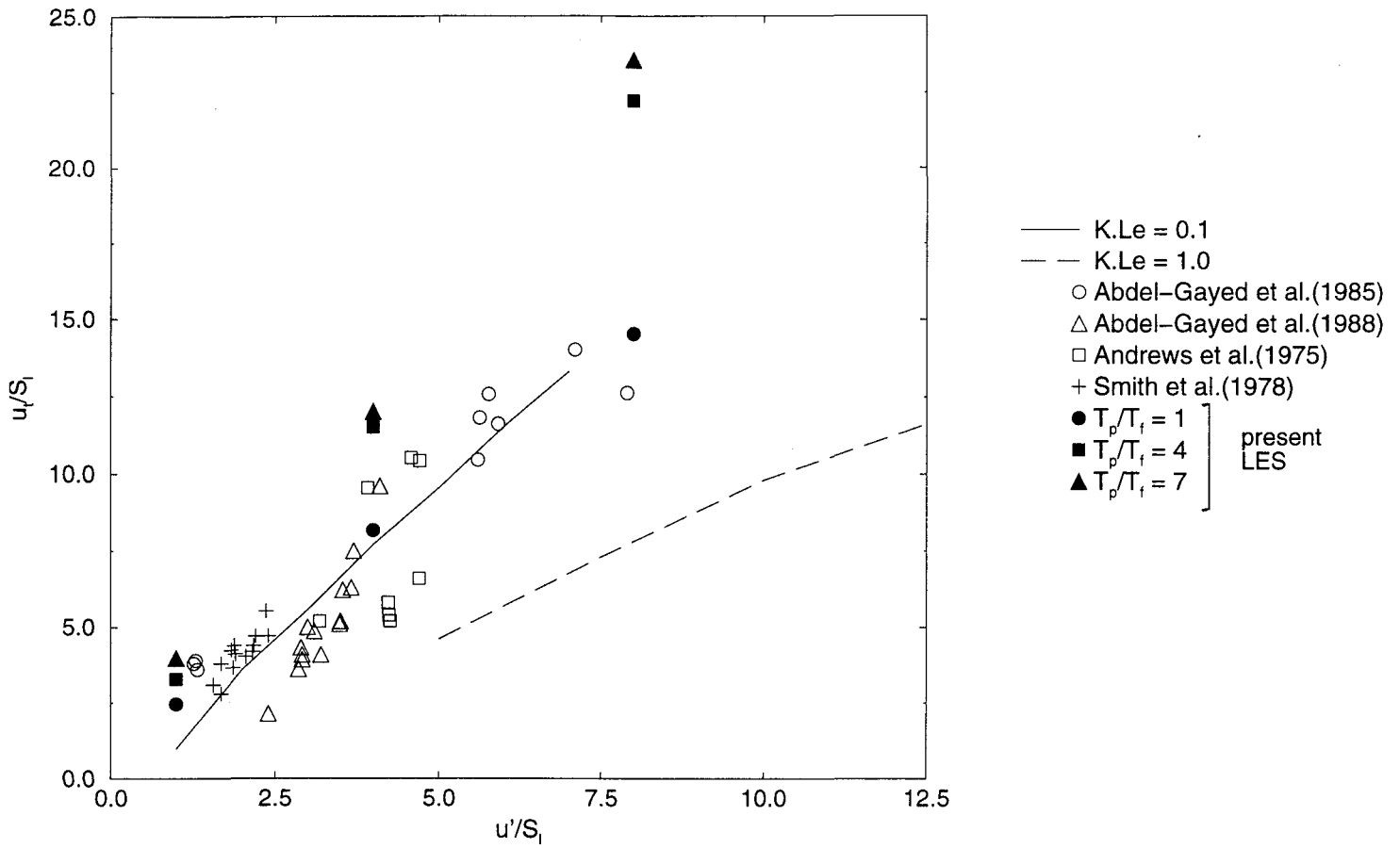


Figure.14 : Comparison of turbulent flame speed predictions with experimental data.  
(K = Karlovitz stretch factor [26], Le = Lewis number)

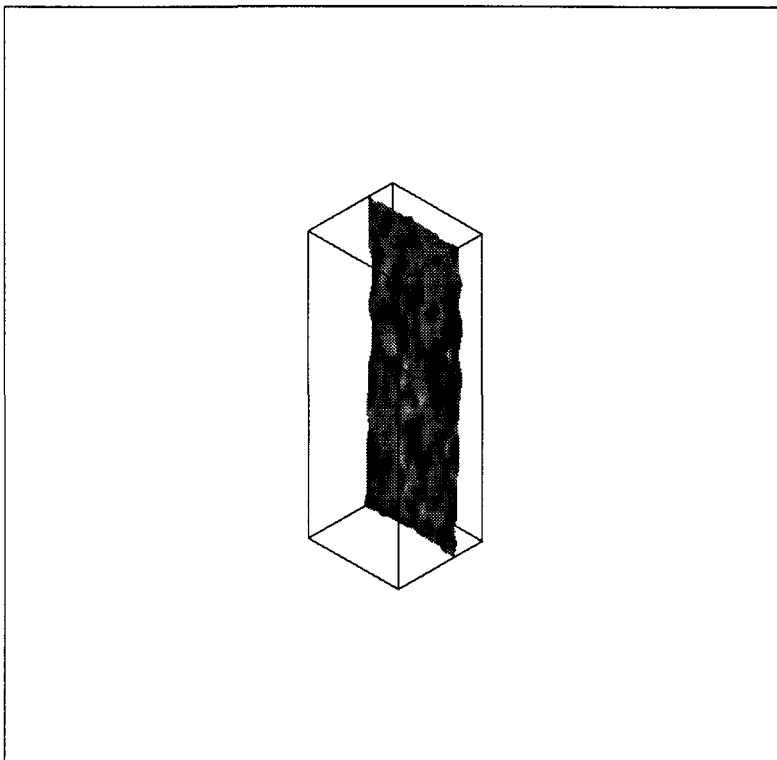


Figure.15 : 3-dimensional structure of the flame in stagnation point flow.

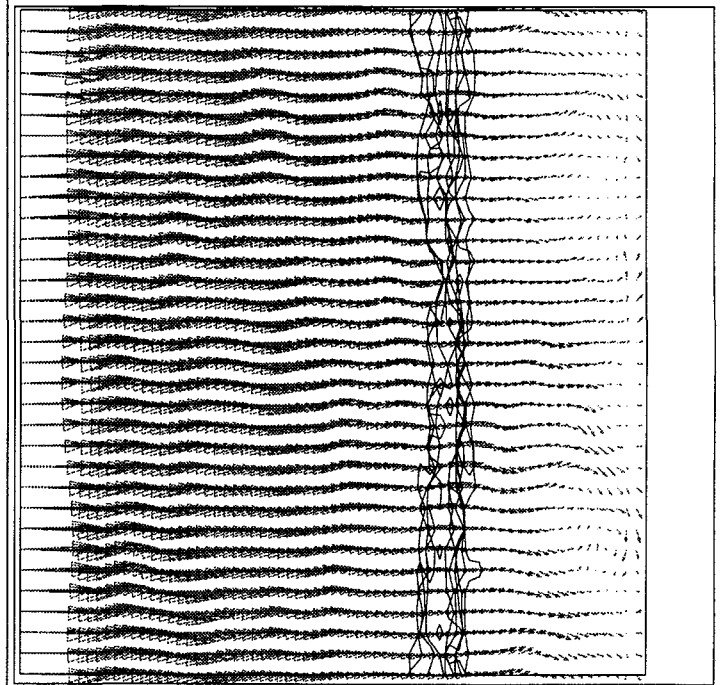


Figure.16 : Superposition of  $G=0.5$  (flame) contours along the homogeneous direction and the instantaneous streak lines.